Evolutionary dynamics of sex chromosomes of palaeognathous birds

Luohao Xu (1), Simon Yung Wa Sin (2,3,4), Phil Grayson (2,3), Daniel E. Janes[†] (3), Scott V. Edwards (2,3), Timothy B. Sackton* (5)

(1) Department of Molecular Evolution and Development, University of Vienna, Austria

(2) Department of Organismic and Evolutionary Biology, Harvard University, USA

(3) Museum of Comparative Zoology, Harvard University, USA

(4) School of Biological Sciences, The University of Hong Kong, Pok Fu Lam Road, Hong Kong

(5) Informatics Group, Harvard University, USA

[†]Current address: National Institutes of Health, 9000 Rockville Pike, Bethesda, MD 20892, USA

*correspondence to: tsackton@g.harvard.edu

Abstract

Standard models of sex chromosome evolution propose that recombination suppression leads to the degeneration of the heterogametic chromosome, as is seen for the Y chromosome in mammals and the W chromosome in most birds. Unlike other birds, palaeognaths (ratites and tinamous) possess large non-degenerate regions on their sex chromosomes (PARs or pseudoautosomal regions), despite sharing the same sex determination region as neognaths (all other birds). It remains unclear why the large PARs of palaeognaths are retained over more than 100 MY of evolution, and the impact of these large PARs on sex chromosome evolution. To address this puzzle, we analysed Z chromosome evolution and gene expression across 12 palaeognaths, several of whose genomes have recently been sequenced. We confirm at the genomic levels that most palaeognaths (excepting some species of tinamous) retain large PARs. As in neognaths, we find that all palaeognaths have incomplete dosage compensation on the regions of the Z chromosome homologous to degenerated portions of the W (differentiated regions or DRs), but we find no evidence for enrichments of male-biased genes in PARs. We find limited evidence for increased evolutionary rates (faster-Z) either across the chromosome or in DRs for most palaeognaths with large PARs, but do recover signals of faster-Z evolution similar to neognaths in tinamou species with mostly degenerated W chromosomes (small PARs). Unexpectedly, in some species PAR-linked genes evolve faster on average than genes on autosomes. Increased TE density and longer introns in PARs of most palaeognaths compared to autosomes suggest that the efficacy of selection may be reduced in palaeognath PARs, contributing to the faster-Z evolution we observe. Our analysis shows that palaeognath Z chromosomes are atypical at the genomic level, but the evolutionary forces maintaining largely homomorphic sex chromosomes in these species remain elusive.

Introduction

Sex chromosomes are thought to evolve from autosomes that acquire a sex determination locus (Bull 1983). Subsequent suppression of recombination between the X and Y (or the Z and W) chromosomes leads to the evolutionary degeneration of the sex-limited (Y or W) chromosome. Theoretical models predict that suppression of recombination will be favored so that the sexually antagonistic alleles that are beneficial in the heterogametic sex can be linked genetically to the sex determination locus (Rice 1987; Ellegren 2011). Recombination suppression is thought to be initiated by inversions, which can occur multiple times in the course of sex chromosome evolution (Lahn and Page 1999; Bergero and Charlesworth 2009; Cortez et al. 2014; Zhou et al. 2014; Wright et al. 2016).

53 Despite differences in their autosomal origins and heterogamety, eutherian mammals and
54 neognathous birds followed similar but independent trajectories of sex chromosome evolution
55 (Graves 2015; Bellott et al. 2017).

56 However, this model of sex chromosome evolution seems incompatible with patterns
57 in many other vertebrate lineages. Henophidian snakes (boas) are thought to have ZW
58 chromosomes that have remained homomorphic for about 100 MY (Vicoso, Emerson, et al.
59 2013), although a recent study suggests a transition from ZW to XY system may have
60 occurred (Gamble et al. 2017). Many lineages in fish and non-avian reptiles also possess
61 homomorphic sex chromosomes, in most cases because the sex chromosomes appear to be
62 young due to frequent sex chromosome turnover (Bachtrog et al. 2014). In some species of
63 frogs, homomorphic sex chromosomes appear to be maintained by occasional XY
64 recombination in sex-reversed XY females (the 'fountain of youth' model), which is possible
65 if recombination suppression is a consequence of phenotypic sex rather than genotype (Perrin
66 2009; Dufresnes et al. 2015; Rodrigues et al. 2018).

67 Palaeognathous birds (Palaeognathae), which include the paraphyletic and flightless
68 ratites and the monophyletic tinamous, and comprise sister group to all other birds, also retain
69 largely or partially homomorphic sex chromosomes (de Boer 1980; Ansari et al. 1988;
70 Ogawa et al. 1998; Nishida-Umehara et al. 1999; Pigozzi and Solari 1999; Stiglec et al. 2007;
71 Tsuda et al. 2007; Janes et al. 2009; Pigozzi 2011), albeit with some exceptions (Zhou et al.
72 2014). These species share the same ancestral sex determination locus, *DMRT1*, with all other
73 birds, suggesting its origin about 150 million years ago (Bergero and Charlesworth 2009;
74 Yazdi and Ellegren 2014). Because recombination occurs in both males and females in birds,
75 the 'fountain of youth' model is also not applicable in this case. Thus, the homomorphic sex
76 chromosomes in palaeognaths must be old.

77 The reasons why palaeognath sex chromosomes have not degenerated are obscure,
78 although two hypotheses have been proposed. Based on an excess of male-biased gene
79 expression in the recombining pseudo-autosomal region, Vicoso and colleagues (Vicoso,
80 Emerson, et al. 2013) suggested that sexual antagonism is resolved by sex-biased expression
81 without recombination suppression and differentiation of Z and W sequences in emu.
82 Alternatively, lack of dosage compensation, which in mammals and other species normalizes
83 expression of genes on the hemizygous chromosome between the homogametic and
84 heterogametic sex, has been proposed as a mechanism that could arrest the degeneration of

85 the W chromosome due to selection to maintain dosage-sensitive genes (Adolfsson and
86 Ellegren 2013). Although these hypotheses are compelling, they have only been tested in
87 single-species studies and without high quality genomes. A broader study of palaeognathous
88 birds is therefore needed for comprehensive understanding of the unusual evolution of their
89 sex chromosomes.

90 Degeneration of sex-limited chromosomes (the W or the Y) leads to the homologous
91 chromosome (the Z or the X) becoming hemizygous in the heterogametic sex. Numerous
92 studies have shown that one common consequence of this hemizygosity is that genes on the
93 X or Z chromosome typically evolve faster on average than genes on the autosomes
94 (Charlesworth et al. 1987; Meisel and Connallon 2013).The general pattern of faster-X or
95 faster-Z protein evolution has been seen in many taxa, including *Drosophila* (Charlesworth et
96 al. 1987; Baines et al. 2008; Avila et al. 2014; Charlesworth et al. 2018), birds (Mank et al.
97 2007; Mank, Nam, et al. 2010), mammals (Torgerson 2003; Lu and Wu 2005; Kousathanas et
98 al. 2014) and moths (Sackton et al. 2014). One primary explanation for this is that recessive
99 beneficial mutations are immediately exposed to selection in the heterogametic sex, leading
100 to more efficient positive selection (Charlesworth et al. 1987; Vicoso and Charlesworth 2006;
101 Mank, Vicoso, et al. 2010). Alternatively, the degeneration of the Y or W chromosomes
102 results in the reduction of the effective population size of the X or Z chromosomes relative to
103 the autosomes (because there are 3 X/Z chromosomes for every 4 autosomes in a diploid
104 population with equal sex ratios). This reduction in the effective population size can increase
105 the rate of fixation of slightly deleterious mutations due to drift (Mank, Vicoso, et al. 2010;
106 Mank, Nam, et al. 2010). In both scenarios, faster evolution of X- or Z-linked genes is
107 expected.

108 The relative importance of these explanations varies across taxa. In both *Drosophila*
109 and mammals, faster evolutionary rates of X-linked genes seem to be driven by more
110 efficient positive selection for recessive beneficial alleles in males (Connallon 2007; Meisel
111 and Connallon 2013). For female-heterogametic taxa, the evidence is mixed. In Lepidoptera
112 there is evidence that faster-Z evolution is also driven by positive selection (Sackton et al.
113 2014) or is absent entirely (Rousselle et al. 2016), whereas in birds, increased fixation of
114 slightly deleterious mutations due to reduced N_e is likely a major factor driving faster-Z
115 evolution (Mank, Nam, et al. 2010; Wang et al. 2014; Wright et al. 2015).

116 The limited degeneration of the W chromosome in palaeognaths makes these species

117 an ideal system to further test the causes of faster-Z evolution in birds. For many
118 palaeognaths, a large proportion of the sex chromosomes retains homology and synteny
119 between the Z and the W; these regions are referred to as pseudoautosomal regions (PARs)
120 because they recombine in both sexes and are functionally not hemizygous in the
121 heterogametic sex. In PARs, no effect of dominance is expected on evolutionary rates, and as
122 the population size of the PAR is not different from that of autosomes, no increase in
123 fixations of weakly deleterious mutations is expected. Therefore, neither the positive
124 selection hypothesis nor the genetic drift hypothesis is expected to lead to differential
125 evolutionary rates in the PAR compared to autosomes, although other selective forces such as
126 sexually antagonistic selection may impact evolutionary rates in the PAR (Otto et al. 2011;
127 Charlesworth et al. 2014).

128 With numerous new palaeognath genomes now available (Zhou et al. 2014; Le Duc et
129 al. 2015; Zhang et al. 2015; Sackton et al. 2018), a reevaluation of sex chromosome evolution
130 in palaeognaths is warranted. Here, we investigate faster-Z evolution, dosage compensation
131 and sex-biased expression, to gain a better understanding of the slow evolution of sex
132 chromosomes in ratites. Surprisingly, we did not find evidence for faster-Z evolution for most
133 palaeognaths, even when analyzing only differentiated regions (DRs) that are functionally
134 hemizygous in the heterogametic sex. Instead, we find limited evidence that PARs tend to
135 evolve faster than autosomes. Indirect evidence from the accumulation of transposable
136 elements and larger introns suggests reduced efficacy of selection in both PARs and DRs,
137 potentially because of lower recombination rates compared to similarly sized autosomes.
138 Based on new and previously published RNA-seq data, we find a strong dosage effect on
139 gene expression, suggesting substantially incomplete dosage compensation as in other birds
140 (Itoh et al. 2010; Adolfsson and Ellegren 2013; Uebbing et al. 2013; Uebbing et al. 2015), but
141 do not recover a previously-reported excess of male-biased expression in the PAR (Vicoso,
142 Kaiser, et al. 2013). Our results suggest that simple models of sex chromosome evolution
143 probably cannot explain evolutionary history of palaeognath sex chromosomes.

144 **Results**

145 **Most palaeognaths have large pseudoautosomal regions**

146 To identify Z-linked scaffolds from palaeognath genomes, we used nucmer (Kurtz et
147 al. 2004) to first align the published ostrich Z chromosome (Zhang et al. 2015) to assembled

148 emu scaffolds (Sackton et al. 2018), and then aligned additional palaeognaths (Fig. 1) to emu.
149 We then ordered and oriented putatively Z-linked scaffolds in non-ostrich assemblies into
150 pseudo-chromosomes using the ostrich Z chromosome as a reference (Fig. S1). Visualization
151 of pseudo-chromosome alignments (Fig. S1) showed little evidence for inter-chromosomal
152 translocations, as expected based on the high degree of synteny across birds (Ellegren 2010);
153 an apparent 12Mb autosomal translocation onto the ostrich Z chromosome is a likely mis-
154 assembly (Fig. S2).

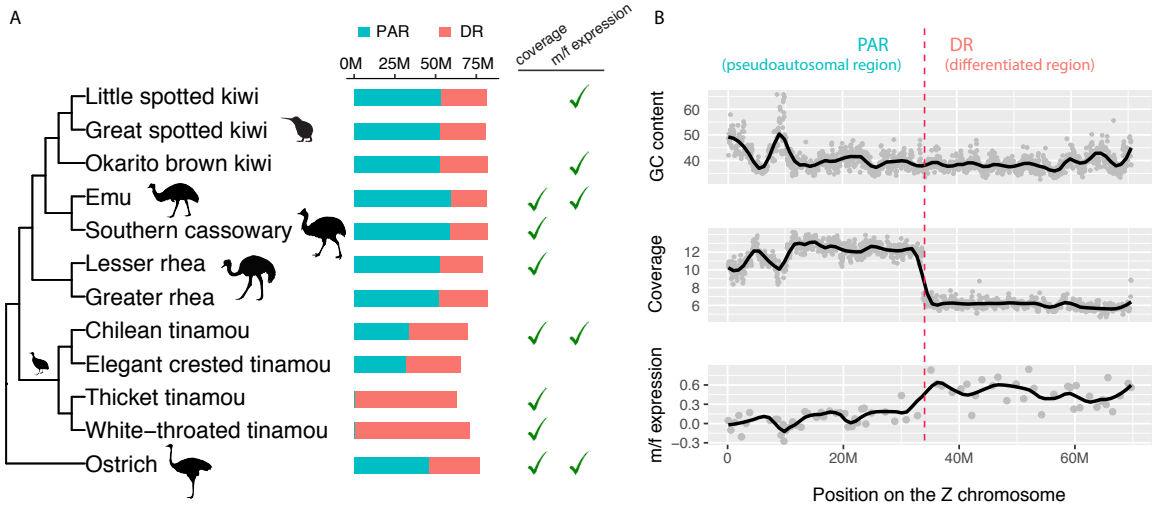

155

FIG. 1. Overview of PAR/DR annotation. **A)** The phylogeny of Palaeognathae based on (Sackton et al. 2018). The sizes of the PARs (pseudoautosomal regions) and DRs (differentiated regions) are indicated by the bars in cyan and tomato. The check marks indicate whether the PAR/DR boundaries were annotated by female read coverage and/or male-to-female expression ratios; species with no checks were annotated by homology to closest relatives. **B)** an example of PAR/DR annotation for Chilean tinamou. In the panels of GC content and coverage depth, each dot represents a 50k window. In the panel of m/f expression, each dot represents log2 transformed mean m/f expression ratio of 10 consecutive genes.

156

157 We next annotated the pseudoautosomal region (PAR) and differentiated region (DR)
158 of the Z chromosome in each species. The DR is thought to arise as a result of inversions on
159 the Z or W chromosome that suppress recombination between the Z and the W, eventually
160 leading to degeneration of the W-linked sequence inside the inversion and hemizygosity of

161 the homologous Z-linked sequence (the DR). Outside the DR – in the PAR – ongoing
162 recombination between the Z and the W chromosome maintains sequence homology. In the
163 DR, reads arising from the W in females will not map to the homologous region of the Z (due
164 to sequence divergence associated with W chromosome degeneration), while in the PAR
165 reads from both the Z and the W will map to the Z chromosome. Thus, we expect coverage of
166 sequencing reads mapped to the Z chromosome in the DR to be ½ that of the autosomes or
167 PAR in females, logically similar to the approach used to annotate Y and W chromosomes in
168 other species (Chen et al. 2012; Carvalho and Clark 2013; Tomaszkiewicz et al. 2017). We
169 also annotated PAR/DR boundaries using gene expression data. If we assume that complete
170 dosage compensation is absence, as it is in all other birds studied to date (Graves 2014), M/F
171 expression ratios of genes on the Z with degenerated W-linked gametologs (in the DR)
172 should be about twice that of genes with intact W-linked gametologs (in the PAR).

173 For seven species genomic sequencing data from females, either newly generated in
174 this study (lesser rhea, thicket tinamou, Chilean tinamou) or previously published (emu,
175 ostrich, cassowary, North Island brown kiwi, white-throated tinamou), we annotated PAR
176 and DR regions using coverage (Fig. 1B, Fig. S3). While some variation in coverage
177 attributable to differences in GC content is apparent, the coverage reduction in the DR region
178 is robust (Fig. 1B). For three of these species, we also used newly generated (emu) or
179 published (ostrich, Chilean tinamou) male and female RNA-seq data; using expression ratios
180 to annotate DR/PAR boundaries produced results consistent with coverage analysis in all
181 three of these species (Fig. 1B, Fig. S3, Fig. S4). We used expression ratios alone to
182 demarcate the DR/PAR boundaries in little spotted kiwi and Okarito kiwi (Fig. S4), which we
183 found to be in similar genomic locations in both species, and also in the same locations as the
184 DR/PAR boundary position in North Island brown kiwi. For three species (greater rhea,
185 elegant crested tinamou and great spotted kiwi) with neither female sequencing data nor
186 expression data, we projected the DR/PAR boundary from a closely related species (lesser
187 rhea, Chilean tinamou and little spotted kiwi respectively). Our results corroborate prior
188 cytogenetic studies across palaeognaths and support a large PAR in all species except the
189 Tinaminae (thicket tinamou and white-throated tinamou), which have small PARs and
190 heteromorphic sex chromosomes. PAR sizes in non-Tinaminae palaeognaths range from 32.2
191 Mb (49% of Z chromosome, in elegant crested tinamou) to 59.3 Mb (73% of Z chromosome,
192 in emu); in contrast, PAR sizes in the Tinaminae and in typical neognaths rarely exceed ~1
193 Mb (~1.3% of Z chromosome size) (Table S1).

194 **Genes with male-biased expression are not overrepresented in palaeognath PARs**

195 Several possible explanations for the maintenance of old, homomorphic sex
196 chromosomes are related to gene dosage (Adolfsson and Ellegren 2013; Vicoso, Kaiser, et al.
197 2013). We analyzed RNA-seq data from males and females from five palaeognath species,
198 including newly collected RNA-seq data from three tissues from emu (brain, gonad, and
199 spleen; 3 biological replicates from each of males and females), as well as previously
200 published RNA-seq data from Chilean tinamou (Sackton et al. 2018), ostrich (Adolfsson and
201 Ellegren 2013), kiwi (Ramstad et al. 2016), and additional embryonic emu samples (Vicoso,
202 Kaiser, et al. 2013). For each species we calculated expression levels for each gene with
203 RSEM (Li and Dewey 2011) and DESeq2 (Love et al. 2014), and computed male/female
204 ratios to assess the extent of dosage compensation, although we note that this measure does
205 not always reflect retention of ancestral sex chromosome expression levels in the hemizygous
206 sex (Gu and Walters 2017). Consistent with previous studies in birds (Graves 2014), we find
207 no evidence for complete dosage compensation by this measure. Instead, we see evidence for
208 partial compensation with M/F ratios ranging from 1.19 to 1.68 (Fig. 2A). The extent of
209 dosage compensation seems to vary among species, but not among tissues within species
210 (Fig. S5).

211 Incomplete dosage compensation poses a challenge for detection of sex-biased genes:
212 higher expression levels of DR-linked genes in males may be due to the incompleteness of
213 dosage compensation rather than sex-biased expression *per se*. With substantially improved
214 genome assemblies (and PAR/DR annotations) and data from a greater number of species, we
215 reevaluated the observation that there is an excess of male-biased genes in the emu PAR.
216 Previous work with a preliminary genome assembly (Vicoso, Kaiser, et al. 2013) showed
217 evidence for an excess of male-biased genes in the emu PAR and argued that sexually
218 antagonistic effects could be resolved via sex-biased expression instead of recombination
219 suppression and W chromosome degeneration.

220

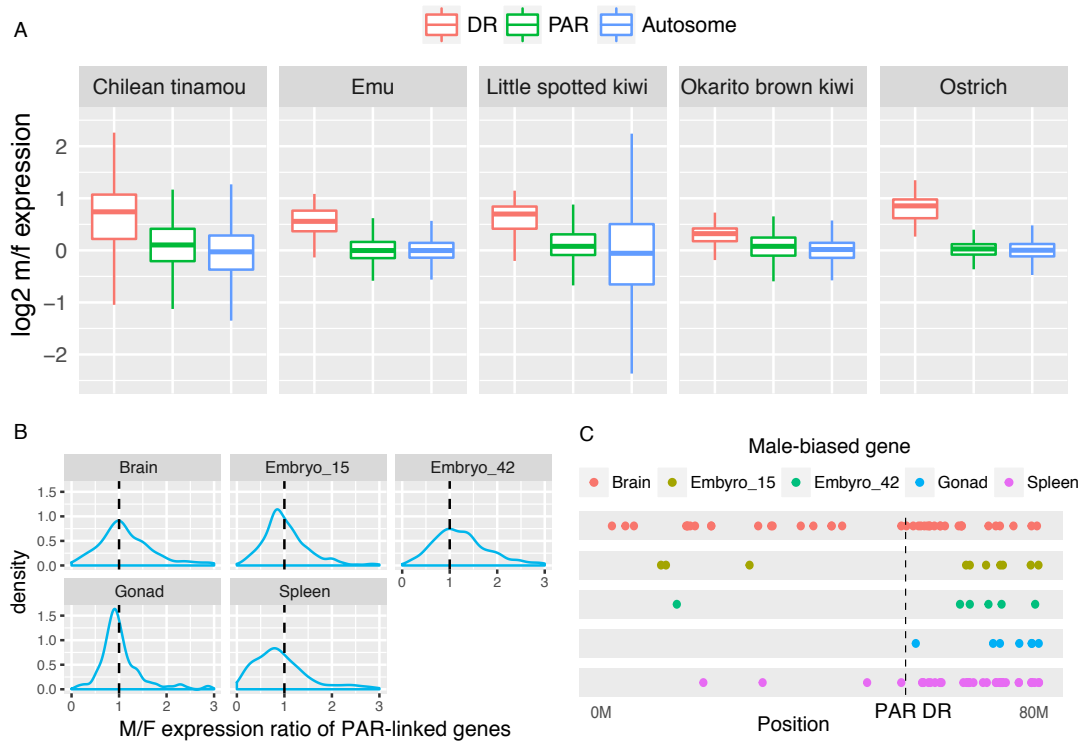

221

222 *FIG. 2*. Transcriptomic analyses for five palaeognathous species. **A)** Incomplete dosage
223 compensation in emu, kiwi and tinamou. For each species, only one sample is shown:
224 Chilean tinamou (brain), emu (gonad), ostrich (brain) and both kiwis have only blood
225 samples. Log2 m/f expression ratios of DR-linked are larger than 0 but lower than 1. **B)** No
226 excess of male expression levels of PAR-linked genes in most emu tissues, despite slight
227 male-biased expression for 42-day embryo. **C)** No over-representation of male-biased genes
228 in emu PAR. Most Z-linked male-biased genes are located on the DR.

229

230 Using the PAR/DR annotation inferred in this study, we analyzed both the previously
231 published RNA-seq data from emu embryos and new RNA-seq data from three biological
232 replicates of three adult tissues from both sexes. We find that most emu Z-linked male-biased
233 genes are located on the DR (Fig. 2C), and when DR genes are excluded, we no longer detect
234 an excess of male-biased genes on the Z chromosome of emu (Fig. 2C). For PAR-linked
235 genes, although there was a slight shift of expression toward male-bias in 42-day emu
236 embryonic brain (Fig. 2B), only one gene was differentially expressed in male (Fig. 2C). This
237 lack of genes with male-biased expression in the PAR is largely consistent across other
238 palaeognaths with large PARs, including Chilean tinamou, ostrich and little spotted kiwi,

239 with one exception in the Okarito brown kiwi (Fig. S6). Overall, we see little evidence for
240 accumulation of male-biased genes in palaeognath PARs, and suggest that the lack of
241 degeneration of the emu W chromosome, and likely other palaeognathous chromosomes is
242 probably not due to resolution of sexual antagonism through acquisition of sex-biased genes.

243 **Large PARs are associated with lack of faster-Z evolution in palaeognaths**

244 The unusually large PARs and the variation in PAR size make Palaeognathae a
245 unique model to study faster-Z evolution. To test whether Z-linked genes evolve faster than
246 autosomal genes, we computed branch-specific dN/dS ratios (the ratio of nonsynonymous
247 substitution rate to synonymous substitution rate) using the PAML free-ratio model for
248 protein coding genes (Yang 2007), based on previously published alignments (Sackton et al.
249 2018). Because macro-chromosomes and micro-chromosomes differ extensively in the rates
250 of evolution in birds (Gossmann et al. 2014; Zhang et al. 2014) (Fig. S7), we include only the
251 macro-chromosomes (chr1 to chr10) in our comparison, and further focus on only
252 chromosome 4 (97 Mb in chicken) and chromosome 5 (63 Mb) to match the size of the Z
253 chromosome, unless otherwise stated.

254 We included include 23 neognaths and 12 palaeognaths in our analysis. Overall, Z-
255 linked genes in neognaths (with few exceptions) have a significantly higher dN/dS ratio than
256 autosomal (chr 4/5) genes, suggesting faster-Z evolution (Fig. 3). This result is consistent
257 with a previous study involving 46 neognaths (Wang et al. 2014). In contrast to neognaths,
258 the majority of palaeognaths, and all but two species with large PARs, had similar dN/dS
259 ratios for autosomal and Z-linked genes, and thus did not show evidence for faster-Z
260 evolution (Fig. 3).

261 The lack of a faster-Z effect for palaeognaths with large PARs is perhaps not surprising, since
262 PAR-linked genes are not expected to evolve faster than autosomal genes under standard
263 models of faster-Z evolution. We divided Z-linked genes into those with presumed intact W-
264 linked gametologs (PAR genes) and those with degenerated W-linked gametologs (DR
265 genes). Surprisingly, we see little evidence for faster-Z evolution in palaeognaths even for
266 DR genes: only in cassowary, thicket tinamou and white-throated tinamou do DR genes show
267 accelerated dN/dS and dN relative to autosomes (Fig. 4, Fig. S8). Thicket tinamou and white-
268 throated tinamou possess small PARs typical of neognaths, and faster-Z has also been

observed for white-throated tinamou in a previous study (Wang et al. 2014), so faster-DR in these species is expected.

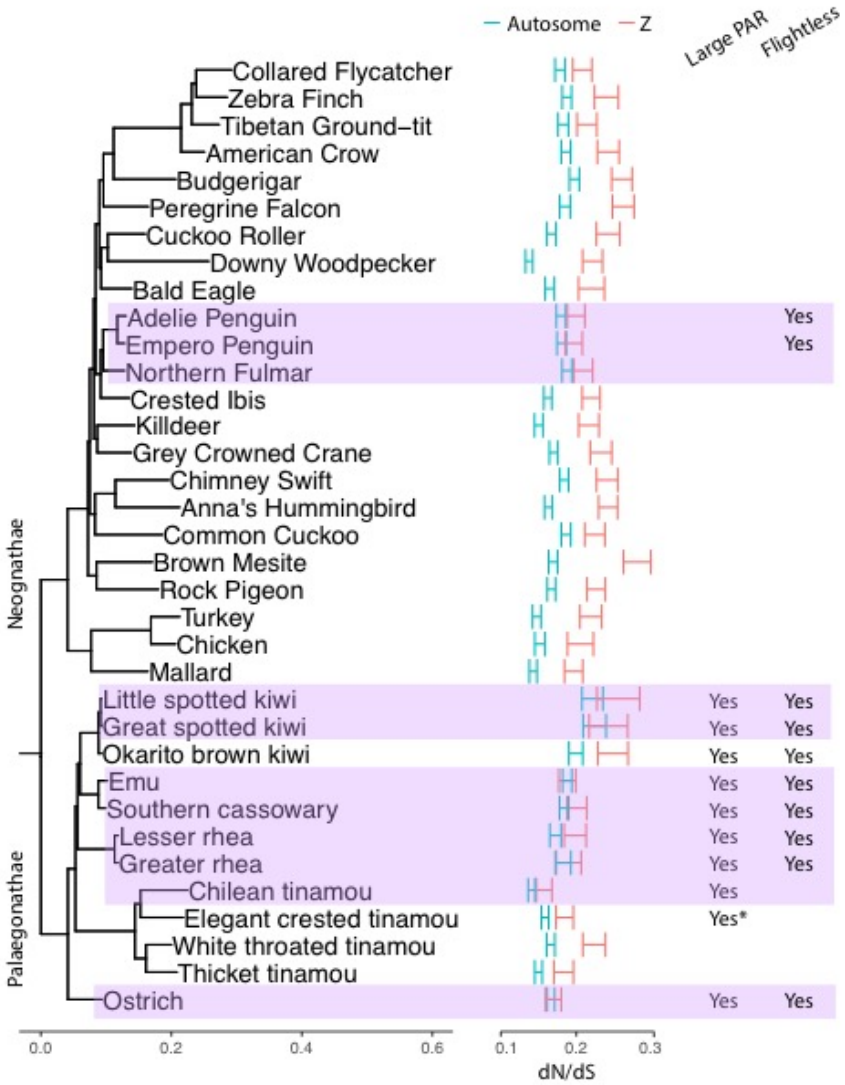

FIG. 3. A lack of faster-Z evolution in most Palaeognaths. Autosomes were represented by chromosome 4 and chromosome 5 (chr4/5) which have similar sizes compared to the Z chromosomes. The confidence intervals of dN/dS ratios were determined by 1,000 bootstraps. Species without faster-Z effect (permutation test, P > 0.05) are highlighted in purple. The asterisk after 'Yes' or 'No' indicates uncertainty.

The observation of faster-DR evolution in cassowary (p = 0.009, two-sided permutation test) suggests that faster-DR evolution may not be limited to species with

extensive degeneration of the W chromosome (e.g., with small PARs). However, an important caveat is that the cassowary genome (alone among the large-PAR species) was derived from a female individual, which means that some W-linked sequence could have been assembled with the Z chromosome, especially for the region with recent degeneration. This would cause an artefactual increase in divergence rate.

Unexpectedly, in four species of palaeognaths we find evidence that genes in the PAR evolve faster than autosomal genes on chromosomes of similar size (chr4/5), which is not predicted by either the positive selection or genetic drift hypothesis for faster-Z evolution (Fig. 4). The faster-PAR effect shows a lineage-specific pattern, particularly in tinamous where three of four species (white-throated tinamou, Chilean tinamou, elegant-crested tinamou) show faster evolution for PAR-linked genes, and all four species have higher dN in the PAR than autosomes, although not significantly so for the elegant-crested tinamou. The faster-PAR in white-throated tinamou is particularly unexpected because previous studies

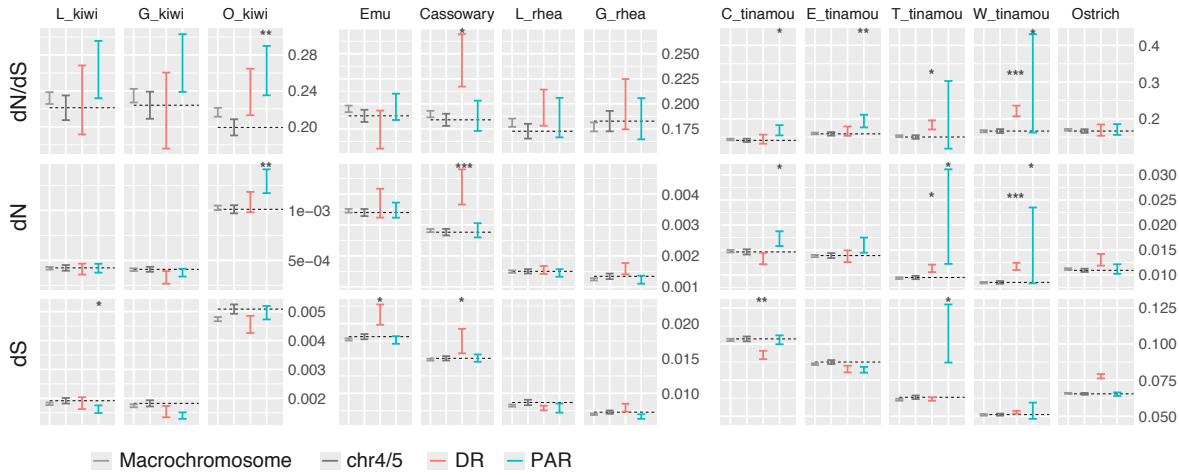

FIG. 4. Relative evolutionary rates of Z-linked and autosomal (chr4/5) genes. Confidence intervals were estimated by 1,000 bootstraps. The label chr4/5 stands for chromosome 4 + chromosome 5, and the median value for chr4/5 is also shown as a dotted line. Asterisks indicate the significant levels of PAR/DR *vs.* chr4/5 comparison (two-sided permutation test), * <0.05, ** <0.01, *** <0.001. Abbreviation for species names: L_kiwi, little spotted kiwi; G_kiwi, great spotted kiwi; O_kiwi, Okarito brown kiwi; L_rhea, Lesser rhea; G_rhea, Greater rhea; C_tinamou, Chilean tinamou; E_tinamou, elegant crested tinamou; T_tinamou, thicket tinamou; W_tinamou, white-throated tinamou.

297

298 suggest that small PARs evolve slower in birds (Smeds et al. 2014). The small number of
299 PAR-linked genes in white-throated tinamou (N=9) suggests some caution in interpreting this
300 trend is warranted. The kiwis also show a trend towards faster-PAR evolution, though this is
301 only statistically significant in Okarito brown kiwi ($p = 0.010$, two-sided permutation test)
302 (Fig. 4). Interestingly, species with evidence for faster-PAR evolution also have suggestive
303 evidence of relatively faster rates of W chromosome degeneration. In particular, tinamous
304 have intermediate or small PARs (Fig. 1), suggesting that sex chromosomes may not be as
305 stable in these species as in ratites. Similarly, while PARs in the little spotted kiwi and great
306 spotted kiwi are large compared to neognaths, they are relatively shorter than in ostrich, emu
307 and cassowary, suggesting additional degeneration of the W chromosomes. Moreover, in
308 North Island brown kiwi, coverage for female reads suggests an on-going degeneration of the
309 W chromosome (Fig. S3). However, further study will be needed to confirm this trend.

310

311 **Evidence for reduced efficacy of selection on the Z chromosome**

312 The signatures of higher dN and dN/dS we observe in the PARs of tinamous and
313 some other species could be driven by increased fixation of weakly deleterious mutations, if
314 the efficacy of selection is reduced in PARs despite homology with the non-degenerated
315 portion of the W chromosome. One potential marker of the efficacy of selection is the density
316 of transposable elements (TEs), which are thought to increase in frequency when the efficacy
317 of selection is reduced (Rizzon et al. 2002; Lockton et al. 2008). We find that chromosome
318 size, which is correlated with recombination rates in birds (Kawakami et al. 2014), shows a
319 strong positive correlation with TE density (lowest in Okarito brown kiwi, $r = 0.90$; highest in
320 white-throated tinamou, $r = 0.98$) (Fig. S9, Table S2). Extrapolating from autosomal data, we
321 would expect PARs (smaller than 50Mb in all species) to have lower TE density than chr5
322 (~63Mb) or chr4 (~89Mb) if similar evolutionary forces are acting on them to purge TEs.
323 Strikingly, we find that all palaeognaths with large PARs harbor significantly higher TE
324 densities on the PAR than autosomes (Fig. 4B), which suggests reduced purging of TEs on
325 PARs. For DRs, it is unsurprising that TE densities are much higher than in chr4/5 (Fig. 4B)
326 since both reduced recombination rates (due to no recombination in females) and reduced N_e
327 (due to hemizygosity of the DR in females) will reduce the efficacy of selection. In fact, TE

328 densities of the DRs are also higher than those of all macro-chromosomes, as well as those of
329 the PARs (Fig. 4B).

330 Intron size is probably also under selective constraint (Carvalho and Clark 1999), and
331 in birds smaller introns are likely favored (Zhang and Edwards 2012; Zhang et al. 2014). If
332 this is also the case in palaeognaths, an expansion of intron sizes could suggest reduced
333 efficacy of selection. We compared the intron sizes among PARs, DRs and autosomes across
334 all palaeognaths in our study. Like TE densities, intron sizes show strong positive correlation
335 with chromosome size (lowest in Okarito brown kiwi, r = 0.74; highest in thicket tinamou, r =
336 0.91) (Fig. S9, Table S2). Except for white-throated tinamou and thicket tinamou, intron sizes
337 of the PARs are larger than those of chr4/5 ($p < 8.8e-10$, Wilcoxon rank sum test, fig. 4C).

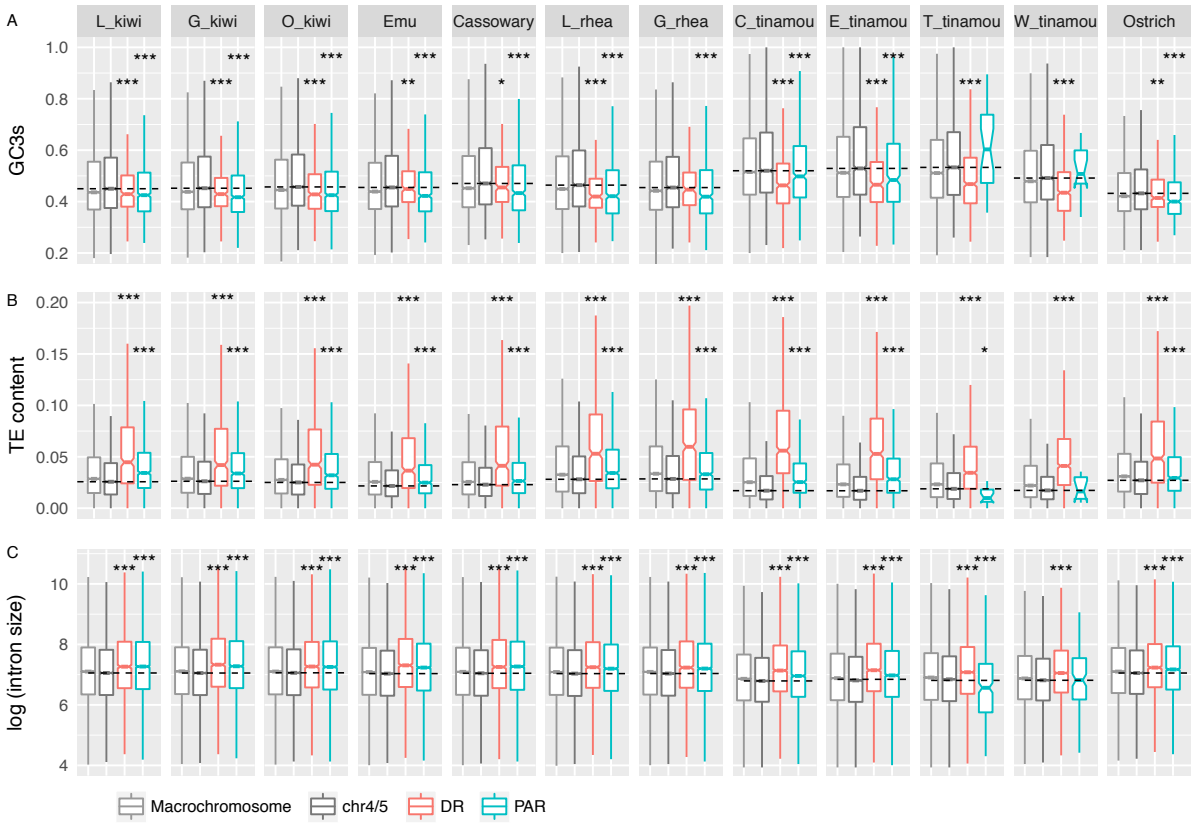

338

339 *FIG. 5.* The comparison of PAR/DR *vs.* chr4/5 and macrochromosomes of four genomic
340 features. Median values from chr/4/5 are shown as a dotted horizontal line. Asterisks indicate
341 the significant levels of PAR/DR *vs.* chr4/5 comparison (Wilcoxon sum rank test), * <0.05,
342 ** <0.01, *** <0.001 **A)** GC content of the synonymous sites. **B)** TE content, including
343 SINE, LINE, LTR and DNA element. **C)** Log transformed intron size.

344 The pattern of larger intron sizes in the PARs remains unchanged when all macro-
345 chromosomes were included for comparison (Fig. S9). Similar to PARs, DRs also show
346 larger intron sizes relative to chr4/5 ($p < 0.00081$, Wilcoxon rank sum test).

347 Finally, codon usage bias is often used as proxy for the efficacy of selection and is
348 predicted to be larger when selection is more efficient (Shields et al. 1988). To assess codon
349 usage bias, we estimated effective number of codon (ENC) values, accounting for local
350 nucleotide composition. ENC is lower when codon bias is stronger, and thus should increase
351 with reduced efficacy of selection. As expected, ENC values showed a strong positive
352 correlation with chromosome sizes (Table S2), and are higher for DR-linked genes in most
353 species (although not rheas, the little spotted kiwi, or the Okarito brown kiwi) (Fig. S10).
354 However, for PAR-linked genes, ENC does not suggest widespread reductions in the efficacy
355 of selection: only cassowary and Chilean tinamou exhibited significantly higher ENC values
356 in the PAR, although a trend of higher ENC values can be seen for most species (Fig. S10).

357 One possible cause of changes in the efficacy of selection in the absence of W
358 chromosome degeneration is a reduction in the recombination rate of the PAR of some
359 species with a large PAR, although a previous study on the collared flycatcher (a neognath
360 species with a very small PAR) showed that the PAR has a high recombination rate (Smeds et
361 al. 2014). Previous work (Bolivar et al. 2016) has shown that recombination rate is strongly
362 positively correlated with GC content of synonymous third positions in codons (GC3s) in
363 birds, so we used GC3s as a proxy for recombination rate in the absent of pedigree or
364 population samples to estimate the rate directly. We find that GC3s are strongly negatively
365 correlated with chromosome size in all palaeognaths (-0.78 ~ -0.91, p-value <= 0.0068)
366 except for ostrich ($r=-0.51$, $p=0.11$) (Fig. S9, Fig. S11, Table S2), similar to what was
367 observed in mammals (Romiguier et al. 2010). Recombination rates are also negatively
368 correlated with chromosome sizes in birds (Gossmann et al. 2014; Kawakami et al. 2014) and
369 other organisms (Jensen-Seaman et al. 2004)(Jensen-Seaman et al. 2004)(Jensen-Seaman et
370 al. 2004)(Jensen-Seaman et al. 2004)(Jensen-Seaman et al. 2004), suggesting that GC3s are at
371 least a plausible proxy for recombination rate. In contrast to the results for collared
372 flycatcher, GC3s of palaeognath PARs were significantly lower than those of chr4/5s ($p <$
373 $2.23e-05$, Wilcoxon sum rank test) (Fig. 5A, Fig. S9, Fig. S11), except for white-throated
374 tinamou and thicket tinamou. Inclusion of the other macro-chromosome does not change the

375 pattern ($p < 0.0034$). Moreover, distribution of GC3s along the PAR is more homogeneous
376 compared to chr4 or chr5, except for the chromosomal ends (Fig. S11).

377 Overall, then, we find evidence from TE density and intron size that efficacy of
378 selection may be reduced on the PAR in most large-PAR palaeognaths, potentially because of
379 reductions in recombination rate (as suggested by reduced GC3s), although we note the
380 signature from codon bias (ENC) is more ambiguous. If indeed recombination rate is reduced
381 relative to a similarly sized autosome for most large-PAR species, that could explain why we
382 see some evidence for faster-PAR evolution in palaeognaths.

383 **Discussion**

384 Old, homomorphic sex chromosomes have long been an evolutionary puzzle, as they
385 defy our usual expectations about how sexually antagonistic selection drives recombination
386 suppression of the Y (or W) chromosome and eventual degradation. A long-standing example
387 of old, homomorphic sex chromosomes are found in the Palaeognathae, where previous
388 cytogenetic and genomic studies have clearly demonstrated the persistence of largely
389 homomorphic sex chromosomes. Our results extend previous studies, and confirm at the
390 genomic level that all ratites and some tinamous have large, nondegenerate PARs, while in at
391 least some Tinaminae degradation of the W chromosome has proceeded, resulting in typically
392 small PARs.

393 **Evolutionary forces acting on sex chromosomes**

394 Several studies have reported evidence for faster-Z evolution in birds, probably driven
395 largely by increased fixation of weakly deleterious mutations due to reduced N_e of the Z
396 chromosome (Mank, Nam, et al. 2010; Wright et al. 2015). However, these studies have
397 focused on neognaths, with fully differentiated sex chromosomes. Here, we show that
398 palaeognath sex chromosomes, which mostly maintain large PARs, do not have consistent
399 evidence for faster-Z evolution, while confirming the pervasive faster-Z effect in neognaths.
400 Notably, the two species in our dataset that presumably share heteromorphic sex
401 chromosomes derived independently from neognaths (white-throated tinamou and thicket
402 tinamou) do show evidence for faster-Z evolution, and in particular faster evolution of DR
403 genes. In contrast, palaeognaths with small DR and large PAR do not tend to show evidence

404 for faster-DR, even though hemizygosity effects should be apparent (the exception is
405 cassowary, which may be an artifact due to W-linked sequence assembling as part of the Z).

406 A previous study on neognaths shows that the increased divergence rate of the Z is
407 mainly contributed by recent strata while the oldest stratum (S0) does not show faster-Z
408 effect (Wang et al. 2014). Neognaths and palaeognaths share the S0, and since their
409 divergence only a small secondary stratum has evolved in palaeognaths (Zhou et al. 2014). In
410 particular, the DR of palaeognaths without heteromorphic sex chromosomes is largely
411 dominated by this shared S0 stratum. The absence of faster-Z effect in palaeognath DR where
412 S0 dominates is therefore largely consistent with the results of the study on the neognath S0
413 stratum. A possible mechanism to explain this pattern is that, in S0, the reduced effective
414 population size (increasing fixation of deleterious mutations) is balanced by the greater
415 efficacy of selection in removing recessive mutations (due to hemizygosity). A recent study
416 on ZW evolution in *Maniola jurtina* and *Pyronia tithonus* butterflies suggests a similar
417 model, where purifying selection is acting on the hemizygous DR genes to remove
418 deleterious mutations (Rousselle et al. 2016). While this model would account for the pattern
419 we observe, it remains unclear why the shared S0 stratum should have a different balance of
420 these forces than the rest of the DR in both neognaths and palaeognaths with large DRs.
421 Nonetheless, the evolutionary rates of the DR genes in the older strata are probably the net
422 results of genetic drift and purifying selection against deleterious mutation, with little
423 contribution of positive selection for recessive beneficial mutations.

424 We also detect evidence for faster evolution of genes in the PAR for tinamous and
425 some species of kiwi. Since the PAR is functionally homomorphic and recombines with the
426 homologous region of the W chromosome, it is not clear why this effect should be observed
427 in these species. However, a common feature of the PARs of tinamous and kiwis is that they
428 are relatively shorter than PARs of other palaeognaths. This raises at least two possible
429 explanations for the faster-PAR effect in tinamous and kiwis: 1) the differentiation of the sex
430 chromosomes is more rapid compared with other palaeognaths, and at least some parts of the
431 PARs may have recently stopped recombining and actually become DR but undetectable by
432 using the coverage method; or 2) the PARs are still recombining but at lower rate, resulting in
433 weaker efficacy of selection against deleterious mutations.

434 **Efficacy of selection and recombination rate**

435 Multiple lines of evidence suggest a possible reduction in the efficacy of selection in
436 the PAR across all palaeognaths with a large PAR. Specifically, we find both an increase in
437 TE density and an increase in intron size in PARs. In contrast, we do not find clear evidence
438 for a reduction in the degree of codon bias in PARs. However, it is possible that genetic drift
439 (Marais et al. 2001), GC-biased gene conversion (Galtier et al. 2018) and/or mutational bias
440 (Szövényi et al. 2017) may also affect the codon bias, which may weaken the correlation
441 between codon usage bias and the strength of natural selection.

442 It is unclear, however, why the efficacy of selection may be reduced in PARs. One
443 possible cause is that the PARs may recombine at lower rate than autosomes. This is a
444 somewhat unexpected prediction because in most species PARs have higher recombination
445 rates than autosomes (Otto et al. 2011). In birds, direct estimates of recombination rates of the
446 PARs are available in both collared flycatcher and zebra finch, and in both species PARs
447 recombines at much higher rates than most macrochromosomes (Smeds et al. 2014; Singhal
448 et al. 2015). This is probably due to the need for at least one obligate crossover in female
449 meiosis, combined with the small size of the PAR in both collared flycatcher and zebra finch.

450 In palaeognaths where PARs are much larger, direct estimates of recombination rate
451 from pedigree or genetic cross data are not available. Our observation that GC3s are
452 significantly lower in large palaeognath PARs than similarly sized autosomes is at least
453 consistent with reduced recombination rates in these species. However, a recent study on
454 greater rhea shows that the recombination rate of the PAR does not differ from similarly
455 sized autosomes in females (del Priore and Pigozzi 2017), but this study did not examine
456 males. Since the recombination rates differ extensively between sexes (van Oers et al. 2014;
457 Halldorsson et al. 2016; Bhérer et al. 2017), more data is needed to test whether sex-average
458 recombination rate of the PAR differs from autosomes. Additionally, a previous study of emu
459 conducted prior to the availability of an emu genome assembly suggested that the PAR has a
460 higher population recombination rate than autosomes (Janes et al. 2009). However, of twenty
461 two loci in that study, seven appear to be incorrectly assigned to the sex chromosomes based
462 on alignment to the emu genome assembly (Table S3), potentially complicating that
463 conclusion. The relatively small size of that study and recently improved resources and
464 refined understanding of recombination rates across chromosome types provide opportunities
465 for a new analysis. Further direct tests of recombination rate on ratite Z chromosomes are
466 needed to resolve these discrepancies.

467

468 **Sexual antagonism and sex chromosome degeneration**

469 A major motivation for studying palaeognath sex chromosomes is that, unusually,
470 many palaeognaths seem to maintain old, homomorphic sex chromosomes. Standard models
471 of sex chromosome evolution, in which recombination suppression evolves in order to tightly
472 link sexually antagonistic mutations to the sex determination locus, thus do not seem to be
473 able to explain palaeognath sex chromosomes. Previous work has suggested two hypotheses
474 to explain this discrepancy: (1) the lack of dosage compensation in birds prevents the
475 degeneration of the W chromosome due to dosage sensitivity (Adolfsson and Ellegren 2013),
476 or (2) sexually antagonistic effects are resolved by the evolution of male-biased expression
477 (Vicoso, Kaiser, et al. 2013).

478 However, neither hypothesis seems to fully explain the slow degeneration of
479 palaeognath sex chromosomes. Published RNA-seq expression data from both males and
480 females from ostrich, Okarito brown kiwi, and little brown kiwi, as well as new RNA-seq
481 data from emu and Chilean tinamou, suggest dosage compensation is partial in palaeognaths
482 and consistent with what has been seen in neognaths. If the absence of complete dosage
483 compensation is the reason for the arrested sex chromosome degeneration in palaeognaths, it
484 is not clear why some palaeognaths (thicket tinamou and white-throated tinamou) and all
485 neognaths have degenerated W chromosomes and small PARs. The other hypothesis, derived
486 from a previous study on emu (Vicoso, Kaiser, et al. 2013), implies an excess of male-biased
487 genes on the PAR as resolution of sexual antagonism. However, gene expression data from
488 multiple tissues and stages of emu show that male-biased genes are only enriched on the DR
489 (presumably attributable to incomplete dosage compensation), with very few present on the
490 PAR. We find similar patterns in other species.

491 Classic views on the evolution of sex chromosomes argue that recombination
492 suppression ultimately leads to the complete degeneration of the sex-limited chromosomes
493 (Charlesworth et al. 2005; Bachtrog 2006). However, recent theoretical work suggests
494 suppression of recombination is not always favored, and may require strong sexually
495 antagonistic selection (Charlesworth et al. 2014) or other conditions (Otto 2014). Thus, there
496 may be conditions which would have driven tight linkage of the sex-determining locus and
497 sex-specific beneficial loci via the suppression of recombination in neognaths (Gorelick et al.

498 2016; Charlesworth 2017), but not in palaeognaths, although it remains unclear the exact
499 model that could produce this pattern (it would require, e.g. fewer sexually antagonistic
500 mutations in palaeognaths).

501 Alternatively, the suppression of recombination between sex chromosomes may be
502 unrelated to sexually antagonistic selection (Rodrigues et al. 2018), and non-adaptive. By
503 model simulations, Cavoto and colleagues (Cavoto et al. 2017) recently suggests complete
504 recombination suppression can sometimes be harmful to the heterogametic sex, and sex
505 chromosomes are not favorable locations for sexually antagonistic alleles in many lineages.
506 An alternative evolutionary explanation for loss of recombination in the heterogametic sex is
507 then needed. Perhaps the rapid evolution of the sex-limited chromosome may have its role in
508 the expansion of the non-recombining region on the sex chromosome. For instance, once
509 recombination ceases around the sex-determination locus, the W (and Y) chromosome
510 rapidly accumulates TEs, particularly LTRs, and the spread of LTRs in the non-recombining
511 region may in turn increase the chance of LTR-mediated chromosomal rearrangements,
512 including inversions, leading to the suppression of recombination between the W and Z (or Y
513 and X). Future study on the W chromosomes of palaeognaths and neognaths is needed to
514 elucidate the role the W in the evolution of avian sex chromosomes.

515 **Methods**

516 **Identification of the Z chromosome, PARs and DRs**

517 The repeat-masked sequence of ostrich Z chromosome (chrZ) (Zhang et al. 2015) was
518 used as a reference to identify the homologous Z-linked scaffolds in recently assembled
519 palaeognath genomes (Sackton et al. 2018). We used nucmer function from MUMmer
520 package (Kurtz et al. 2004) to first align the ostrich Z-linked scaffolds to emu genome; an
521 emu scaffold was defined as Z-linked if more than 50% of the sequence was aligned. The Z-
522 linked scaffolds of emu were further used as reference to infer the homologous Z-linked
523 sequences in the other palaeognaths because of the more continuous assembly of emu
524 genome and closer phylogenetic relationships, and 60% coverage of alignment was required.
525 During this process, we found that a ~12Mb genomic region of ostrich chrZ (scf347, scf179,
526 scf289, scf79, scf816 and a part of scf9) aligned to chicken autosomes. The two breakpoints
527 can be aligned to a single scaffold of lesser rhea (scaffold_0) (Fig. S1), so we checked
528 whether there could be a mis-assembly in ostrich by mapping the 10k and 20k mate-pair
529 reads from ostrich to the ostrich assembly. We inspected the reads alignments around the
530 breakpoint and confirmed a likely mis-assembly (Fig. S2). The homologous sequences of this
531 region were subsequently removed from palaeognathous Z-linked sequences. When a smaller
532 ostrich scaffold showed discordant orientation and/or order, but its entire sequence was
533 harbored within the length of longer scaffolds of other palaeognaths (Fig. S1), we manually
534 changed the orientation and/or order of that scaffold for consistency. After correcting the
535 orientations and orders of ostrich scaffolds of chrZ, a second round of nucmer alignment was
536 performed to determine the chromosomal positions for palaeognathous Z-linked scaffolds.

537 One way to infer the boundary between the PAR (pseudoautosomal region) and DR
538 (differentiated region) is to compare the differences of sequencing depth of female DNA.
539 Because the DR is not recombining in female and W-linked DR will degenerate over time
540 (and thus diverge from Z-linked DR), the depth of sequencing reads from the Z-linked DR is
541 generally expected to be half of that from the PAR or autosomes. This approach was applied
542 to cassowary, whose sequence is derived a female individual. For emu, female sequencing
543 was available from Vicoso et al. (Vicoso, Kaiser, et al. 2013). To facilitate the PAR
544 annotation, we generated additional DNA-seq data from a female for each of lesser rhea,
545 Chilean tinamou and thicket tinamou. Default parameters of BWA (v0.7.9) were used to map
546 DNA reads to the repeat-masked genomes with BWA-MEM algorithm (Li 2013), and

547 mapping depth was calculated by SAMtools (v1.2) (Li et al. 2009). A fixed sliding window
548 of 50kb was set to calculate average mapping depths along the scaffolds. Any windows
549 containing less than 5kb were removed. Significant shifts of sequencing depth were annotated
550 as the boundaries of the PARs and DRs.

551 Another independent method for PAR annotation is based on gene expression
552 differences between male and female of PAR- and DR-linked genes. To reduce the effect of
553 transcriptional noise and sex-biased expression, 20-gene windows were used to calculate the
554 mean male-to-female ratios. The shifts of male-to-female expression ratios were used to
555 annotate approximate PAR/DR boundaries. This method was applied to little spotted kiwi,
556 Okarito brown kiwi, emu and Chilean tinamou. Given the small divergence between little
557 spotted kiwi and great spotted kiwi, it is reasonable to infer that the latter should have a
558 similar PAR size. Neither female reads nor RNA-seq reads are available for greater rheas and
559 elegant crested tinamou, so the PAR/DR boundaries of lesser rhea and Chilean tinamou were
560 used to estimate the boundaries respectively.

561 **Comparison of genomic features**

562 To estimate GC content of synonymous sites of the third position of codons (GC3s),
563 codonW (http://codonw.sourceforge.net) was used with the option '-gc3s'. The exon density
564 was calculated by dividing the total length of exon over a fixed 50k windows by the window
565 size. Similarly, we summed the lengths of transposable elements (TEs, including LINE,
566 SINE, LTR and DNA element) based on RepeatMasker outputs (Kapusta *et al*, personal
567 communication) to calculate density for 50k windows. Intron sizes were calculated from gene
568 annotations (GFF file). Codon usage bias were quantified by effective number of codons
569 (ENC) using ENCprime. We used intronic sequences to estimate background nucleotide
570 frequency to further reduce the effect of local GC content on codon usage estimates.
571 Wilcoxon sum rank test were used to assess statistical significance.

572 **Divergence analyses**

573 The estimates of synonymous and non-synonymous substitution numbers and sites
574 were extracted from PAML (Yang 2007) outputs generated by free-ratio branch models,
575 based on alignments produced by Sackton et al (Sackton et al. 2018). For a given
576 chromosome, the overall synonymous substitution rate (dS) was calculated as the ratio of the

577 number of synonymous substitution to the number of synonymous site over the entire
578 chromosome, similarly, the chromosome-wide dN was calculated using the numbers of non-
579 synonymous substitution and site over the entire chromosome (this is effectively a length-
580 weighted average of individual gene values). The dN/dS values (ω) were calculated by the
581 ratios of dN to dS values. Confidence intervals for dN, dS and dN/dS were estimated using
582 the R package 'boot' with 1000 replicates of bootstrapping. P-values were calculated by
583 taking 1000 permutation tests.

584 **Gene expression analyses**

585 Three biological replicates of samples from emu brains, gonads and spleens of both
586 adult sexes were collected from Songline Emu farm (specimen numbers: Museum of
587 Comparative Zoology, Harvard University Cryo 6597-6608). For Chilean tinamou, RNA
588 samples were collected from brains and gonads of both sexes of adults with one biological
589 replicate (raw data from (Sackton et al. 2018), but re-analyzed here). RNA-seq reads for both
590 sexes of ostrich brain and liver (Adolfsson and Ellegren 2013), emu embryonic brains of two
591 stages (Vicoso, Kaiser, et al. 2013), and blood of little spotted kiwi and Okarito brown kiwi
592 (Ramstad et al. 2016) were downloaded from NCBI.

593 For the newly generated samples (emu brains, gonads and spleens), RNA extraction
594 was performed using RNeasy Plus Mini kit (Qiagen). The quality of the total RNA was
595 assessed using the RNA Nano kit (Agilent). Poly-A selection was conducted on the total
596 RNA using PrepX PolyA mRNA Isolation Kit (Takara). The mRNA was assessed using the
597 RNA Pico kit (Agilent) and used to make transcriptome libraries using the PrepX RNA-Seq
598 for Illumina Library Kit (Takara). HS DNA kit (Agilent) was used to assess the library
599 quality. The libraries were quantified by performing qPCR (KAPA library quantification kit)
600 and then sequenced on an NextSeq instrument (High Output 150 kit, PE 75 bp reads). Each
601 library was sequenced to a depth of approximately 30M reads. The quality of the RNA-seq
602 data was assessed using FastQC. Error correction was performed using Rcorrector; unfixable
603 reads were removed. Adapters were removed using TrimGalore!. Reads of rRNAs were
604 removed by mapping to the Silva rRNA database.

605 We used RSEM (v1.2.22) (Li and Dewey 2011) to quantify the gene expression
606 levels. RSEM implemented bowtie2 (v2.2.6) to map the RNA-seq raw reads to transcripts
607 (based on a GTF file for each species), and default parameters were used for expression

608 quantification. TPM (Transcripts Per Million) on the gene level were used to represent the
609 normalized expression. The expected reads counts rounded from RSEM outputs were used as
610 inputs for DESeq2 (Love et al. 2014) for differential expression analysis between sexes. We
611 used a 5% FDR cutoff to considered as sex-biased genes.

612

613 **Acknowledgements**

614 We thank John Parsch, Beatriz Vicoso, and Qi Zhou for their useful comments. The
615 computations in this paper were performed on the Odyssey cluster at Harvard University and
616 supported by Harvard University Research Computing. This work was supported by NSF
617 grant DEB-135343/EAR-1355292 to SVE. All raw data newly generated in this study (emu
618 RNA-seq, and DNA-seq from lesser rhea, Chilean tinamou, and thicket tinamou) are
619 available from NCBI at BioProjects XXXXXX and XXXXXX.

620 **References**:

621 Adolfsson S, Ellegren H. 2013. Lack of dosage compensation accompanies the arrested stage
622 of sex chromosome evolution in ostriches. Mol. Biol. Evol. 30:806–810.
623 Ansari HA, Takagi N, Sasaki M. 1988. Morphological differentiation of sex chromosomes in
624 three species of ratite birds. Cytogenet. Genome Res. 47:185–188.
625 Avila V, Marion de Procé S, Campos JL, Borthwick H, Charlesworth B, Betancourt AJ.
626 2014. Faster-X effects in two Drosophila lineages. Genome Biol. Evol. 6:2968–2982.
627 Bachtrog D. 2006. A dynamic view of sex chromosome evolution. Curr. Opin. Genet. Dev.
628 16:578–585.
629 Bachtrog D, Mank JE, Peichel CL, Kirkpatrick M, Otto SP, Ashman T-L, Hahn MW, Kitano
630 J, Mayrose I, Ming R, et al. 2014. Sex determination: why so many ways of doing it? PLoS
631 Biol. 12:e1001899.
632 Baines JF, Sawyer SA, Hartl DL, Parsch J. 2008. Effects of X-Linkage and Sex-Biased Gene
633 Expression on the Rate of Adaptive Protein Evolution in Drosophila. Mol. Biol. Evol.
634 25:1639–1650.
635 Bergero R, Charlesworth D. 2009. The evolution of restricted recombination in sex
636 chromosomes. Trends Ecol. Evol. 24:94–102.
637 Bhérer C, Campbell CL, Auton A. 2017. Refined genetic maps reveal sexual dimorphism in

638 human meiotic recombination at multiple scales. Nat. Commun. 8:14994.
639 de Boer LE. 1980. Do the chromosomes of the kiwi provide evidence for a monophyletic
640 origin of the ratites? Nature 287:84–85.
641 Bolivar P, Mugal CF, Nater A, Ellegren H. 2016. Recombination Rate Variation Modulates
642 Gene Sequence Evolution Mainly via GC-Biased Gene Conversion, Not Hill-Robertson
643 Interference, in an Avian System. Mol. Biol. Evol. 33:216–227.
644 Bull JJ. 1983. Evolution of sex determining mechanisms. Benjamin-Cummings Publishing
645 Company
646 Carvalho AB, Clark AG. 1999. Genetic recombination: Intron size and natural selection.
647 Nature 401:344–344.
648 Carvalho AB, Clark AG. 2013. Efficient identification of Y chromosome sequences in the
649 human and Drosophila genomes. Genome Res. 23:1894–1907.
650 Cavoto E, Neuenschwander S, Goudet J, Perrin N. 2017. Sex-antagonistic genes, XY
651 recombination and feminized Y chromosomes. J. Evol. Biol. 65:123.
652 Charlesworth B, Campos JL, Jackson BC. 2018. Faster-X evolution: theory and evidence
653 from Drosophila. Mol. Ecol.
654 Charlesworth B, Coyne JA, Barton NH. 1987. The relative rates of evolution of sex
655 chromosomes and autosomes. Am. Nat.
656 Charlesworth B, Jordan CY, Charlesworth D. 2014. The evolutionary dynamics of sexually
657 antagonistic mutations in pseudoautosomal regions of sex chromosomes. Evolution 68:1339–
658 1350.
659 Charlesworth D. 2017. Evolution of recombination rates between sex chromosomes. Philos.
660 Trans. R. Soc. Lond. B. Biol. Sci. 372:20160456.
661 Charlesworth D, Charlesworth B, Marais G. 2005. Steps in the evolution of heteromorphic
662 sex chromosomes. Heredity 95:118–128.
663 Chen N, Bellott DW, Page DC, Clark AG. 2012. Identification of avian W-linked contigs by
664 short-read sequencing. BMC Genomics 13:183.
665 Connallon T. 2007. Adaptive Protein Evolution of X-linked and Autosomal Genes in
666 Drosophila: Implications for Faster-X Hypotheses. Mol. Biol. Evol. 24:2566–2572.
667 Cortez D, Marin R, Toledo-Flores D, Froidevaux L, Liechti A, Waters PD, Grützner F,
668 Kaessmann H. 2014. Origins and functional evolution of Y chromosomes across mammals.
669 Nature 508:488–493.
670 Dufresnes C, Borzée A, Horn A, Stöck M, Ostini M, Sermier R, Wassef J, Litvinchuck SN,
671 Kosch TA, Waldman B, et al. 2015. Sex-Chromosome Homomorphy in Palearctic Tree Frogs

672 Results from Both Turnovers and X–Y Recombination. Mol. Biol. Evol. 32:2328–2337.
673 Ellegren H. 2010. Evolutionary stasis: the stable chromosomes of birds. Trends Ecol. Evol.
674 25:283–291.
675 Ellegren H. 2011. Sex-chromosome evolution: recent progress and the influence of male and
676 female heterogamety. Nat. Rev. Genet. 12:157–166.
677 Galtier N, Roux C, Rousselle M, Romiguier J, Figuet E, Glemin S, Bierne N, Duret L. 2018.
678 Codon usage bias in animals: disentangling the effects of natural selection, effective
679 population size and GC-biased gene conversion. Mol. Biol. Evol.
680 Gamble T, Castoe TA, Nielsen SV, Banks JL, Card DC, Schield DR, Schuett GW, Booth W.
681 2017. The Discovery of XY Sex Chromosomes in a Boa and Python. Curr. Biol.:1–11.
682 Gorelick R, Fraser D, Mansfield M, Dawson JW, Wijenayake S, Bertram SM. 2016. Abrupt
683 shortening of bird W chromosomes in ancestral Neognathae. Biol. J. Linn. Soc. 119:488–496.
684 Gossmann TI, Santure AW, Sheldon BC, Slate J, Zeng K. 2014. Highly variable
685 recombinational landscape modulates efficacy of natural selection in birds. Genome Biol.
686 Evol. 6:2061–2075.
687 Graves JAM. 2014. Avian sex, sex chromosomes, and dosage compensation in the age of
688 genomics. Chromosome Res. 22:45–57.
689 Graves JAM. 2015. Evolution of vertebrate sex chromosomes and dosage compensation. Nat.
690 Rev. Genet. 17:33–46.
691 Gu L, Walters JR. 2017. Evolution of Sex Chromosome Dosage Compensation in Animals: A
692 Beautiful Theory, Undermined by Facts and Bedeviled by Details. Genome Biol. Evol.
693 9:2461–2476.
694 Halldorsson BV, Hardarson MT, Kehr B, Styrkarsdottir U, Gylfason A, Thorleifsson G, Zink
695 F, Jonasdottir A, Jonasdottir A, Sulem P, et al. 2016. The rate of meiotic gene conversion
696 varies by sex and age. Nat. Genet. 48:1377–1384.
697 Itoh Y, Replogle K, Kim Y-H, Wade J, Clayton DF, Arnold AP. 2010. Sex bias and dosage
698 compensation in the zebra finch versus chicken genomes: general and specialized patterns
699 among birds. Genome Res. 20:512–518.
700 Janes DE, Ezaz T, Marshall Graves JA, Edwards SV. 2009. Recombination and Nucleotide
701 Diversity in the Sex Chromosomal Pseudoautosomal Region of the Emu, Dromaius
702 novaehollandiae. J. Hered. 100:125–136.
703 Jensen-Seaman MI, Furey TS, Payseur BA, Lu Y, Roskin KM, Chen C-F, Thomas MA,
704 Haussler D, Jacob HJ. 2004. Comparative recombination rates in the rat, mouse, and human
705 genomes. Genome Res. 14:528–538.

706 Kawakami T, Smeds L, Backström N, Husby A, Qvarnström A, Mugal CF, Olason P,
707 Ellegren H. 2014. A high-density linkage map enables a second-generation collared
708 flycatcher genome assembly and reveals the patterns of avian recombination rate variation
709 and chromosomal evolution. Mol. Ecol. 23:4035–4058.
710 Kousathanas A, Halligan DL, Keightley PD. 2014. Faster-X Adaptive Protein Evolution in
711 House Mice. Genetics 196:1131–1143.
712 Kurtz S, Phillippy A, Delcher AL, Smoot M, Shumway M, Antonescu C, Salzberg SL. 2004.
713 Versatile and open software for comparing large genomes. Genome Biol. 5:R12.
714 Lahn BT, Page DC. 1999. Four Evolutionary Strata on the Human X Chromosome. Science
715 286:964–967.
716 Le Duc D, Renaud G, Krishnan A, Almén MS, Huynen L, Prohaska SJ, Ongyerth M,
717 Bitarello BD, Schiöth HB, Hofreiter M, et al. 2015. Kiwi genome provides insights into
718 evolution of a nocturnal lifestyle. Genome Biol.:1–15.
719 Li B, Dewey CN. 2011. RSEM: accurate transcript quantification from RNA-Seq data with or
720 without a reference genome. BMC Bioinformatics 12:323.
721 Li H. 2013. Aligning sequence reads, clone sequences and assembly contigs with BWA-
722 MEM. ArXiv13033997 Q-Bio [Internet]. Available from: http://arxiv.org/abs/1303.3997
723 Li H, Handsaker B, Wysoker A, Fennell T, Ruan J, Homer N, Marth G, Abecasis G, Durbin
724 R. 2009. The Sequence Alignment/Map format and SAMtools. Bioinformatics 25:2078–
725 2079.
726 Lockton S, Ross-Ibarra J, Gaut BS. 2008. Demography and weak selection drive patterns of
727 transposable element diversity in natural populations of Arabidopsis lyrata. Proc. Natl. Acad.
728 Sci. U. S. A. 105:13965–13970.
729 Love MI, Huber W, Anders S. 2014. Moderated estimation of fold change and dispersion for
730 RNA-seq data with DESeq2. Genome Biol. 15:550.
731 Lu J, Wu C-I. 2005. Weak selection revealed by the whole-genome comparison of the X
732 chromosome and autosomes of human and chimpanzee. Proc. Natl. Acad. Sci. 102:4063–
733 4067.
734 Mank JE, Axelsson E, Ellegren H. 2007. Fast-X on the Z: Rapid evolution of sex-linked
735 genes in birds. Genome Res. 17:618–624.
736 Mank JE, Nam K, Ellegren H. 2010. Faster-Z Evolution Is Predominantly Due to Genetic
737 Drift. Mol. Biol. Evol. 27:661–670.
738 Mank JE, Vicoso B, Berlin S, Charlesworth B. 2010. EFFECTIVE POPULATION SIZE
739 AND THE FASTER-X EFFECT: EMPIRICAL RESULTS AND THEIR

740 INTERPRETATION. Evolution 64:663–674.
741 Marais G, Mouchiroud D, Duret L. 2001. Does recombination improve selection on codon
742 usage? Lessons from nematode and fly complete genomes. Proc. Natl. Acad. Sci. 98:5688–
743 5692.
744 Meisel RP, Connallon T. 2013. The faster-X effect: integrating theory and data. Trends
745 Genet. 29:537–544.
746 Nishida-Umehara C, Fujiwara A, Ogawa A, Mizuno S, Abe S, Yoshida MC. 1999.
747 Differentiation of Z and W chromosomes revealed by replication banding and FISH mapping
748 of sex-chromosome-linked DNA markers in the cassowary (Aves, Ratitae). Chromosome
749 Res. 7:635–640.
750 van Oers K, Santure AW, De Cauwer I, van Bers NEM, Crooijmans RPMA, Sheldon BC,
751 Visser ME, Slate J, Groenen MAM. 2014. Replicated high-density genetic maps of two great
752 tit populations reveal fine-scale genomic departures from sex-equal recombination rates.
753 Heredity 112:307–316.
754 Ogawa A, Murata K, Mizuno S. 1998. The location of Z- and W-linked marker genes and
755 sequence on the homomorphic sex chromosomes of the ostrich and the emu. Proc. Natl.
756 Acad. Sci. 95:4415–4418.
757 Otto SP. 2014. Selective maintenance of recombination between the sex chromosomes. J.
758 Evol. Biol. 27:1431–1442.
759 Otto SP, Pannell JR, Peichel CL, Ashman T-L, Charlesworth D, Chippindale AK, Delph LF,
760 Guerrero RF, Scarpino SV, McAllister BF. 2011. About PAR: The distinct evolutionary
761 dynamics of the pseudoautosomal region. Trends Genet. 27:358–367.
762 Perrin N. 2009. Sex reversal: a fountain of youth for sex chromosomes? Evol. Int. J. Org.
763 Evol. 63:3043–3049.
764 Pigozzi MI. 2011. Diverse stages of sex-chromosome differentiation in tinamid birds:
765 evidence from crossover analysis in Eudromia elegans and Crypturellus tataupa. Genetica
766 139:771–777.
767 Pigozzi MI, Solari AJ. 1999. The ZW pairs of two paleognath birds from two orders show
768 transitional stages of sex chromosome differentiation. :1–11.
769 del Priore L, Pigozzi MI. 2017. Broad-scale recombination pattern in the primitive bird Rhea
770 americana (Ratites, Palaeognathae). PLoS ONE 12:e0187549.
771 Ramstad KM, Miller HC, Kolle G. 2016. Sixteen kiwi (Apteryx spp) transcriptomes provide
772 a wealth of genetic markers and insight into sex chromosome evolution in birds. BMC
773 Genomics 17:410.

774 Rice WR. 1987. THE ACCUMULATION OF SEXUALLY ANTAGONISTIC GENES AS
775 A SELECTIVE AGENT PROMOTING THE EVOLUTION OF REDUCED
776 RECOMBINATION BETWEEN PRIMITIVE SEX CHROMOSOMES. Evolution 41:911–
777 914.
778 Rizzon C, Marais G, Gouy M, Biémont C. 2002. Recombination rate and the distribution of
779 transposable elements in the Drosophila melanogaster genome. Genome Res. 12:400–407.
780 Rodrigues N, Studer T, Dufresnes C, Perrin N. 2018. Sex-chromosome recombination in
781 common frogs brings water to the fountain-of-youth. Mol. Biol. Evol. 67:1.
782 Romiguier J, Ranwez V, Douzery EJP, Galtier N. 2010. Contrasting GC-content dynamics
783 across 33 mammalian genomes: relationship with life-history traits and chromosome sizes.
784 Genome Res. 20:1001–1009.
785 Rousselle M, Faivre N, Ballenghien M, Galtier N, Nabholz B. 2016. Hemizygosity Enhances
786 Purifying Selection: Lack of Fast-Z Evolution in Two Satyrine Butterflies. Genome Biol.
787 Evol. 8:3108–3119.
788 Sackton TB, Corbett-Detig RB, Nagaraju J, Vaishna L, Arunkumar KP, Hartl DL. 2014.
789 Positive selection drives faster-Z evolution in silkmoths. Evolution 68:2331–2342.
790 Sackton TB, Grayson P, Cloutier A, Hu Z, Liu JS, Wheeler NE, Gardner PP, Clarke JA,
791 Baker AJ, Clamp M, et al. 2018. Convergent regulatory evolution and the origin of
792 flightlessness in palaeognathous birds. bioRxiv:262584.
793 Shields DC, Sharp PM, Higgins DG, Wright F. 1988. " Silent" sites in Drosophila genes are
794 not neutral: evidence of selection among synonymous codons. Mol. Biol. Evol. 5:704–716.
795 Singhal S, Leffler EM, Sannareddy K, Turner I, Venn O, Hooper DM, Strand AI, Li Q,
796 Raney B, Balakrishnan CN, et al. 2015. Stable recombination hotspots in birds. Science
797 350:928–932.
798 Smeds L, Kawakami T, Burri R, Bolivar P, Husby A, Qvarnström A, Uebbing S, Ellegren H.
799 2014. Genomic identification and characterization of the pseudoautosomal region in highly
800 differentiated avian sex chromosomes. Nat. Commun. 5:5448.
801 Stiglec R, Ezaz T, Graves JAM. 2007. A new look at the evolution of avian sex
802 chromosomes. Cytogenet. Genome Res. 117:103–109.
803 Szövényi P, Ullrich KK, Rensing SA, Lang D, van Gessel N, Stenøien HK, Conti E, Reski R.
804 2017. Selfing in Haploid Plants and Efficacy of Selection: Codon Usage Bias in the Model
805 Moss Physcomitrella patens. Genome Biol. Evol. 9:1528–1546.
806 Tomaszkiewicz M, Medvedev P, Makova KD. 2017. Y and W Chromosome Assemblies:
807 Approaches and Discoveries. Trends Genet.:1–17.

808 Torgerson DG. 2003. Sex-Linked Mammalian Sperm Proteins Evolve Faster Than
809 Autosomal Ones. Mol. Biol. Evol. 20:1705–1709.
810 Tsuda Y, Nishida-Umehara C, Ishijima J, Yamada K, Matsuda Y. 2007. Comparison of the Z
811 and W sex chromosomal architectures in elegant crested tinamou (Eudromia elegans) and
812 ostrich (Struthio camelus) and the process of sex chromosome differentiation in
813 palaeognathous birds. Chromosoma 116:159–173.
814 Uebbing S, Konzer A, Xu L, Backström N, Brunström B, Bergquist J, Ellegren H. 2015.
815 Quantitative Mass Spectrometry Reveals Partial Translational Regulation for Dosage
816 Compensation in Chicken. Mol. Biol. Evol. 32:2716–2725.
817 Uebbing S, Künstner A, Mäkinen H, Ellegren H. 2013. Transcriptome sequencing reveals the
818 character of incomplete dosage compensation across multiple tissues in flycatchers. Genome
819 Biol. Evol. 5:1555–1566.
820 Vicoso B, Charlesworth B. 2006. Evolution on the X chromosome: unusual patterns and
821 processes. Nat. Rev. Genet. 7:645–653.
822 Vicoso B, Emerson JJ, Zektser Y, Mahajan S, Bachtrog D. 2013. Comparative Sex
823 Chromosome Genomics in Snakes: Differentiation, Evolutionary Strata, and Lack of Global
824 Dosage Compensation. PLoS Biol. 11:e1001643–15.
825 Vicoso B, Kaiser VB, Bachtrog D. 2013. Sex-biased gene expression at homomorphic sex
826 chromosomes in emus and its implication for sex chromosome evolution. Proc. Natl. Acad.
827 Sci. 110:6453–6458.
828 Wang Z, Zhang J, Yang W, An N, Zhang P, Zhang G, Zhou Q. 2014. Temporal genomic
829 evolution of bird sex chromosomes. :1–12.
830 Wright AE, Dean R, Zimmer F, Mank JE. 2016. How to make a sex chromosome. Nat.
831 Commun. 7:1–8.
832 Wright AE, Harrison PW, Zimmer F, Montgomery SH, Pointer MA, Mank JE. 2015.
833 Variation in promiscuity and sexual selection drives avian rate of Faster-Z evolution. Mol.
834 Ecol. 24:1218–1235.
835 Yang Z. 2007. PAML 4: Phylogenetic Analysis by Maximum Likelihood. Mol. Biol. Evol.
836 24:1586–1591.
837 Yazdi HP, Ellegren H. 2014. Old but not (so) degenerated–slow evolution of largely
838 homomorphic sex chromosomes in ratites. Mol. Biol. Evol. 31:1444–1453.
839 Zhang G, Li C, Li Q, Li B, Larkin DM, Lee C, Storz JF, Antunes A, Greenwold MJ,
840 Meredith RW, et al. 2014. Comparative genomics reveals insights into avian genome
841 evolution and adaptation. Science 346:1311–1320.

842 Zhang J, Li C, Zhou Q, Zhang G. 2015. Improving the ostrich genome assembly using optical
843 mapping data. GigaScience 4:298–3.
844 Zhang Q, Edwards SV. 2012. The Evolution of Intron Size in Amniotes: A Role for Powered
845 Flight? Genome Biol. Evol. 4:1033–1043.
846 Zhou Q, Zhang J, Bachtrog D, An N, Huang Q, Jarvis ED, Gilbert MTP, Zhang G. 2014.
847 Complex evolutionary trajectories of sex chromosomes across bird taxa. Science
848 346:1246338.
849